

# Link-Layer Salvaging for Making Routing Progress in Mobile Ad Hoc Networks

Chansu Yu  
Department of Electrical and  
Computer Engineering  
Cleveland State University  
Cleveland, OH 44115  
c.yu91@csuohio.edu

Kang G. Shin  
Department of Electrical Engineering  
and Computer Science  
University of Michigan  
Ann Arbor, MI 48109  
kgshin@eecs.umich.edu

Lubo Song  
Department of Electrical and  
Computer Engineering  
Cleveland State University  
Cleveland, OH 44115  
l.song2@csuohio.edu

## ABSTRACT

IEEE 802.11 MAC, called the Distributed Coordination Function (DCF), employs carrier sensing to effectively avoid collisions, but this makes it difficult to maximally reuse the spatial spectral resource available for exposed terminals. This paper proposes a new MAC algorithm, called *Multiple Access with Salvation Army (MASA)*, which adopts less sensitive carrier sensing to promote more spatial reuse of the channel. However, this may result in a higher collision probability. MASA alleviates this problem by adaptively adjusting the communication distance via “packet salvaging” at the MAC layer. Extensive simulation based on the ns-2 has shown MASA to offer as much as 25% higher packet delivery rate and 27% higher throughput than the DCF with the CBR (constant bit rate) and TCP traffic, respectively. In particular, a significant reduction in packet delay, 86% and 70% lower packet delay with the CBR and TCP traffic, makes MASA suitable for delay-sensitive applications. For practicality, we discuss the implementation of MASA based on the DCF specification.

## Categories and Subject Descriptors

C.2.1 [Network Architecture and Design]: Wireless Communication

## General Terms

Algorithms, Design, Theory

## Keywords

Mobile ad hoc networks, carrier sense, medium access control, capture effect, non-deterministic algorithm

## 1. INTRODUCTION

Path loss in wireless communication fundamentally limits the performance of mobile ad hoc networks by requiring intermediate relay nodes to participate in delivery of data packets, but it creates a new opportunity for distant nodes in the

network to reuse the shared radio channel simultaneously. However, since simultaneous data transfers increase aggregate co-channel interference, it is also important to make sure that each data transfer “survives” in the presence of other interfering data transfers.

*Carrier sense (CS)* based *medium access control (MAC)* algorithms alleviate the interference problem by mandating a node to hold up pending transmission requests when it observes a carrier signal above the *CS threshold* [1]. A lower CS threshold will result in less interference and thus a better signal-to-interference-ratio (SIR) at the receiver. However, the low CS threshold may have a negative impact on network capacity because it allows a fewer concurrent data transfers in the network. Therefore, the CS threshold should be configured to balance between the spatial reusability and the interference problem [14]. Two other important factors in this regard are communication distance and *capture effect* [35]. For example, in a land mobile radio environment where the signal strength attenuates as the fourth power of the distance, halving the communication distance results in a 16 times stronger signal at the receiver, meaning that the communication becomes much more robust to interference. If communication distance is short, the low CS threshold would be an overkill because the SIR is high enough anyway.

Advantage of short communications in a multihop environment has been reported in literature. Grossglauser and Tse concluded in [8] that the network capacity can be maximized by allocating the channel to the nodes that can communicate over short distance. In their proposed algorithm, each sender buffers the data traffic until its destination node approaches near it. Similarly, De Couto *et al.* observed that shortest (hop count) path does not always provide the best performance because this path usually consists of longer hop communications, each of which is easily subjective to interference with low radio link quality or a small SIR [6]. More recently, researchers have proposed variations of IEEE 802.11 DCF [11] that speculates on the outcome of a transmission based on signal strength and communication distance. For instance, Xu and Gerla proposed a *Conservative Clear-to-Send Reply (CCR)* scheme [29] in which a node replies only for a Request-to-Send (RTS) when the receiving power of the RTS is higher than a certain threshold, ensuring that the sender is in the proximity of the receiver. Ye *et al.* proposed an *aggressive virtual carrier sensing (AVCS)* scheme [32] that allows a node to start its communication, which

Permission to make digital or hard copies of all or part of this work for personal or classroom use is granted without fee provided that copies are not made or distributed for profit or commercial advantage and that copies bear this notice and the full citation on the first page. To copy otherwise, or republish, to post on servers or to redistribute to lists, requires prior specific permission and/or a fee.

MobiHoc '05, May 25–27, 2005, Urbana-Champaign, Illinois, USA.

Copyright ACM 1-59593-004-3/05/0005...\$5.00.

is prohibited by the virtual CS using the RTS-CTS handshake, when the communication distance is short. However, these schemes have a limited practical value because most of the routing algorithms developed for wireless ad hoc networks offer shortest paths for a given source-destination pair and thus, the physical distance for each hop is usually in the order of maximum transmit range supported by the radio hardware.

This paper presents a non-deterministic MAC algorithm, called the *Multiple Access with Salvation Army (MASA)*, that adopts a higher CS threshold to encourage more spatial reuse but adjusts the communication distance on-the-fly by salvaging packets at the MAC layer to mitigate the interference problem. A key idea is that even if an intended receiver could not receive a data packet due to interference, a third party node among those in between the sender and the receiver, called the *salvation army*, “captures” or “salvages” the packet and makes progress toward the receiver. While packet salvaging is not new at the network layer [12, 22], MASA operates at the MAC layer for faster salvaging. It is also different from other non-deterministic MAC layer schemes [2, 3, 10, 26, 36] in the following two respects.

- It is purely a MAC-layer scheme. While cross-layer design has been discussed in the literature [7], the layered network architecture still has its clear advantages. For example, the MASA algorithm can be integrated with any routing protocols. This paper uses *Dynamic Source Routing (DSR)* [12] and *Ad-hoc On-demand Distance Vector (AODV)* [22] for its evaluation.
- It uses a deterministic routing path whenever possible, and salvages packets only when the primary path breaks. This makes the proposed MASA protocol more attractive in a variety of mobile environments. For example, when traffic intensity is light, MASA does not salvage packets and simply uses the shortest paths because the collision probability is low.

The rest of the paper is structured as follows. Section 2 discusses related work including previous packet-salvaging schemes at the network and MAC layers. It also discusses the other throughput-enhancing techniques such as *transmit power control (TPC)* and *transmit rate control (TRC)*. Section 3 presents the system model including the DCF and the radio propagation model that determines packet capturing. Section 4 analyzes the maximum network throughput in terms of CS threshold and communication distance. The proposed packet-salvaging MAC algorithm, called MASA, is presented in Section 5. Extensive simulation based on ns-2 [20] has been conducted to evaluate various performance metrics such as packet delay, packet delivery ratio, routing control overhead, and packet queueing requirement, which are reported in Section 6. Section 7 draws conclusions and describes future directions of this study.

## 2. RELATED WORK

Section 2.1 and 2.2 overview network- and MAC-layer packet-salvaging schemes, respectively. Section 2.3 briefly discusses the TPC and TRC schemes and their merits and demerits.

### 2.1 Packet Salvaging at the Network Layer

Ad hoc network routing protocols are designed to primarily cope with relatively infrequent but permanent link errors. However,

they may not perform well with more frequent, random and temporary link errors. The former is caused by node mobility but the latter is in part attributed to congestion and collisions. A temporary link breakage may cause a serious performance impact when it is misinterpreted as a permanent link error. A number of packets already in flight could be lost and a routing protocol, *e.g.*, DSR [12], would initiate a new route-discovery procedure that basically floods the network with control messages, which makes the situation worse or the problem to persist longer.

This motivates consideration of non-deterministic routing solutions, where temporary link breakages can be handled on a temporary basis, *i.e.*, a routing path is pre-calculated but can optionally be determined on-the-fly when the primary path is not available. In DSR, an optimization technique known as “packet salvaging” [12] is used so that the node encountered the forwarding failure may search its local storage for alternative routes. If a route is found, it is used to forward the undeliverable packets without resorting to an expensive route-discovery procedure. The “local repair” mechanism in the AODV routing protocol [22] does a similar thing. Valera *et al.* suggested a distributed packet salvaging scheme for more improvement [28]: Every node maintains a small buffer for caching data packets that pass through it, and at least two routes to every active destination. When a downstream node encounters a forwarding error, an upstream node with an alternative route as well as the pertinent data in its buffer can be used to retransmit the data packets.

However, the above-mentioned packet-salvaging schemes do not keep the sender from initiating an expensive route-discovery procedure since their original goal is to save packets in flight. Moreover, these schemes kick in only after a lower-level protocol has attempted for a number of times without a success. For example, the DCF [14] retransmits four times before the link error is reported to the higher-level protocol. Each retransmission not only wastes resources such as node energy and channel resource but also extends the packet delay. Shortest-path routing protocols aggravate the situation because they prefer longer per-hop communication distance, and the corresponding wireless links are more prone to temporary breakages.

### 2.2 Packet Salvaging at the MAC Layer

Non-deterministic packet salvaging at the MAC layer has received significant attention recently to deal with frequent, temporary link errors quickly and efficiently [2, 3, 10, 26, 36]. Biswas and Morris proposed *Extremely Opportunistic Routing (ExOR)*, which defers the choice of the next-hop node among the pre-computed candidates until after the previous node has transmitted the packet via its radio interface [2]. Based on the number of hops to the final destination and the past history of delivery ratios, the sender prioritizes the candidates and includes the list in the packet header. Each candidate competes to become a receiver by delaying its reply for the amount of time determined by its priority in the list.

Blum *et al.* proposed *Implicit Geographic Forwarding (IGF)* which is also a non-deterministic algorithm [3]. Like in *Geographic Forwarding (GF)* [15], the sender has position information of its neighbors as well as the final destination node

of its packet. However, unlike in GF, the choice of the next-hop node is not determined by the sender but by competition among the candidates as in the ExOR scheme. The sender transmits an *Open RTS* (no intended receiver is specified) and each candidate delays its response (Clear-to-Send or CTS) for an amount of time determined by the distance to the destination and the remaining node energy.

Zorzi and Rao presented *Geographic Random Forwarding (GeRaF)*, which is basically the same as IGF but the competition is coordinated by the sender with two control messages, called CONTINUE and COLLISION, in addition to RTS and CTS messages [36]. Here, the transmission coverage area of a sender, only in the direction of the final destination, is divided into a number of regions. When a sender transmits an RTS, any node in the closest region to the destination responds with a CTS. When no CTS is heard, the sender transmits a CONTINUE message so that the nodes in the next region can respond. When more than one CTS are sent, the sender hears a signal but is unable to detect a meaningful message. In this case, the sender transmits a COLLISION message, which will trigger a collision-resolution algorithm [36].

In *Stateless Non-deterministic Geographic Forwarding (SNGF)* algorithm, which is part of the sensor network protocol *SPEED* [10], each node computes the forwarding candidate set for each destination, a member node of which is a neighbor and is closer to the destination than the node itself. Location information of the node as well as the destination is necessary in SNGF.

In the *Distributed Passive Routing Decisions* [26] protocol, routing decisions are made by the potential receivers to elect the optimal node as the receiver. The transmitter sends out an RTS which includes the location information of the transmitter and the final destination. Each potential receiver calculates its optimality and maps this into a backoff delay. The final routing decision is made through the receiver competition.

The above-mentioned schemes depend either on location information [3, 10, 26, 36] or use a link-state flooding scheme [2] to help determine the salvager among multiple candidates, which may not be feasible in real implementations. The goal of this paper is to develop a practical non-deterministic MAC algorithm that requires neither the location information nor the link state propagation.

### 2.3 Transmit Power and Rate Control

TPC allows a node to adjust and optimize its radio transmit power to reach the receiver node but not more than that. A key benefit of the TPC schemes is energy conservation but it also reduces interference allowing more concurrent data transfers. A major problem with the TPC scheme is that it creates *asymmetric links* where one end-node can reach the other, but not the other way around [33]. The asymmetric links render the MAC-layer protocol such as the DCF as well as network-layer protocols such as AODV and DSR inoperable because control packets implementing these protocols usually work only on symmetric links. For this reason, most of TPC-based protocols [13, 19] are concerned primarily with low power transmission of data packets and assume that control packets are transmitted at the highest radio power. Therefore, they do not directly increase the spatial

reusability of the spectral resource. On the contrary, *Smallest Common Power* (COMPOW) [19] and *Power-Stepped Protocol* (PSP) [33] use the same radio power for both data and control packets but they incur an additional overhead to compute the optimal transmit power level.

TRC exploits a physical-layer multi-rate capability to make a data transfer more robust to interference. Since Shannon's theorem provides the maximum achievable data rate for a given SIR, a lower-rate communication can be successful even if the SIR is not high. For example, a receiver measures the channel quality based on the RTS message transmitted from the sender and then informs the appropriate transmit rate to the sender so that the channel can always be utilized at the highest feasible data rate. Shepard showed the theoretic bounds of the network throughput, assuming that the transmit rate is arbitrarily adjustable [25]. Prabhakar *et al.* proposed an energy-efficient communication schedule that takes the TRC capability into account [23]. And Sadeghi *et al.* proposed an opportunistic media access scheme that better exploits the channel via TRC and channel quality information [24]. More recently, Yang and Vaidya showed via analysis and simulation that TRC can significantly improve the overall network throughput [31]. In summary, when a node experiences packet collision, it can lower the data rate to improve performance.

Although the TRC and TPC schemes can be integrated with the proposed MASA algorithm when the corresponding hardware capability is available, we leave it as one of our future work and assume that radios use the same transmit power and rate in this paper.

## 3. SYSTEM MODEL

As discussed in the Introduction, carrier sensing is used to avoid unwanted interferences, but it potentially limits the spatial channel utilization in wireless ad hoc networks. This section discusses the radio-propagation model and the DCF with a special focus on its spatial reusability.

### 3.1 Radio-Propagation Model

Propagation in the mobile channel is described by means of three effects: *attenuation* due to distance ( $d$ ) between the sender (node  $i$ ) and the receiver (node  $j$ ), *shadowing* due to the lack of visibility between the two nodes, and *fading* due to multipath propagation [35]. This paper assumes a simple propagation model by considering only the path loss due to communication distance. According to the *two-ray ground propagation model*, the mean received signal power ( $P_r$ ) follows an inverse distance power loss law, where an exponent  $\alpha$  assumes values between 2 and 4, and is typically 4 in land mobile radio environments [35]. In other words,  $P_r = P_{t,i} \gamma_{ij}$ , where  $P_{t,i}$  is the radio transmit power of node  $i$  and  $\gamma_{ij} \propto d^{-\alpha}$  is the channel gain from node  $i$  to node  $j$ . In the 915 MHz WaveLAN radio hardware, the transmit power is 24.5 dBm and the receive sensitivity is -72 dBm, which is translated to 250m or shorter distance between the sender and the receiver ( $d$ ) for successful communication [4, 27].

When another node (say, node  $k$ ) in node  $j$ 's proximity attempts to transmit during the communication between node  $i$  and  $j$ , it may cause collision at the receiver (node  $j$ ) and thus, both data

transfers would fail. However, collision does not necessarily destroy all packets involved and one of them may survive if the received signal power is far greater than that of the interfering signal. This is one of the key features in a mobile radio environment known as *capture effect* [35]. In general, in order for node  $j$  to receive a signal from node  $i$  correctly, the instantaneous signal to noise ratio must be larger than a certain threshold, called *capture ratio* or  $z_0$ , which is determined by the sensitivity and capability of the radio receiver circuitry, *i.e.*,

$$SIR = \frac{P_{t,i}\gamma_{ij}}{N_0 + \sum_{k \neq i} P_{t,k}\gamma_{kj}} > z_0 \quad (1)$$

where  $N_0$  is the background noise power.  $z_0$  ranges from 1 (perfect capture) to  $\infty$  (no capture) [35].

### 3.2 DCF (IEEE 802.11 MAC)

A MAC protocol for multi-access media is essentially a distributed scheduling algorithm that allocates the available spectral resource to requesting nodes. In general, the performance of a MAC protocol is greatly affected by collisions because a packet transmission to a busy receiver is not queued but incurs transmission failures for both packets. Thus, in order for a sender to transmit a packet successfully, other interfering nodes within a receiver's reception area, called *vulnerable space* (VS) [33], should not attempt to transmit during the sender's transmission, which is referred to as *vulnerable period* [16]. On the other hand, the spatial area, which could have been used for other communications but is wasted due to excessive CS, is called *wasted space* (WS) in this paper. A MAC algorithm should reduce VS but at the same time should reduce WS, too. In the below, we will discuss how VS and WS are related to CS threshold, receive sensitivity, and capture threshold. They are directly translated to *CS zone*, *transmission zone*, and *capture (CP) zone*, respectively, which will be discussed in more detail later in this and the following sections.

Carrier-sensing protocols shrink the VS by suppressing the neighboring nodes of the transmitter. When node  $i$  transmits a data packet to node  $j$  as in Fig. 1(a), the CS zone of the sender (node  $i$ ), denoted as  $CS_i$ , is a circular region in which a node would observe the sender's signal to be higher than the CS threshold. Thus, nodes in  $CS_i$  would not attempt to cause interference to the communication between nodes  $i$  and  $j$ . In other words,  $VS = \overline{CS_i}$ .

The DCF optionally employs the *RTS/CTS* (*Request-to-Send* and *Clear-to-Send*) handshake to further reduce collisions. By overhearing two short control packets, every neighboring node of the  $i$ - $j$  communication recognizes the transmission and keeps it from sending its own transmission. This is known as *virtual carrier sensing* (VCS) [11] and the VS is now reduced to  $\overline{CS_i \cup TR_j}$  as shown in Fig. 1(b). Here,  $TR_j$  is the transmission zone of node  $j$ , *i.e.*, any node in  $TR_j$  can receive node  $j$ 's transmission, such as CTS.

The DCF works reasonably well in infra-structured one-hop networks. However, in wireless multihop networks, the carrier sensing and the RTS/CTS handshake creates WS and thus, the

exposed terminal problem. It may cause a live link to be considered broken when an intended receiver is unnecessarily exposed to other pair's communication and thus cannot respond to RTS. In summary, the carrier sensing and the RTS/CTS handshake are effective in combating collisions (VS), but they may have a negative impact on performance by reserving unnecessarily large space (WS).

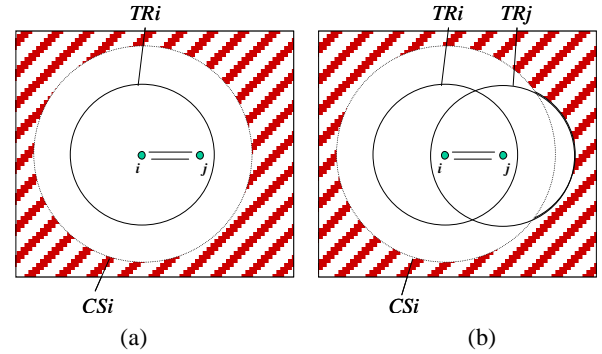


Figure 1. Vulnerable space (hatched area) in the DCF. (a) With CS, and (b) With CS and RTS/CTS.

## 4. THROUGHPUT ANALYSIS OF MULTIHOP NETWORK

In order to see the effect of communication distance and carrier sensing, this section presents the throughput analysis of multihop networks. Analyses without considering the effect of carrier sensing can be found in [8, 9, 25]. Recently, Zhu *et al.* extended the analysis to find the optimal CS threshold that maximizes the spatial utilization [34]. Yang and Vaidya extended it further by including the MAC overhead [31]. Xu *et al.* [29] analyzed the effectiveness of VCS in terms of communication distance and CS threshold. Our analysis is different from theirs in that we take the effect of multiple interferers as well as communication distance and CS threshold into account. In this section, a perfect MAC-layer coordination is assumed where the medium access is perfectly scheduled without overhead and collisions as similarly assumed in [8, 9]. Section 4.1 considers the case with a single interferer and Section 4.2 provides the maximum network throughput with multiple interferers.

### 4.1 VS and WS Analysis with a Single Interferer

Assuming that  $N_0$  is ignorable and the transmit power is constant, equation (1) for a single interfering node  $k$  becomes

$$SIR = \frac{P_{t,i}\gamma_{ij}}{P_{t,k}\gamma_{kj}} = \frac{\gamma_{ij}}{\gamma_{kj}} = \frac{d^{-\alpha}}{D^{-\alpha}} = \left(\frac{D}{d}\right)^\alpha > z_0 \quad \text{or} \quad D > z_0^{1/\alpha} d \quad (2)$$

where  $d$  and  $D$  denote the sender-to-receiver ( $i$ - $j$ ) and interferer-to-receiver ( $k$ - $j$ ) distance, respectively, as shown in Fig. 2. Equation (2) defines the *capture zone* of node  $j$  denoted as  $CP_j$ . Any node outside of  $CP_j$  does not cause collisions to the  $i$ - $j$  communication due to capture effect, *i.e.*,  $D_{min} = z_0^{1/\alpha} d$  for a successful communication. It means that  $VS = \overline{CP_j \cap (CS_i \cup TR_j)}$ , which is marked as the hatched area on the right in Fig. 2. On the other hand, the capture effect causes the WS nonempty that

has been reserved via carrier sensing but does not need to be protected. That is,  $WS = (CS_i \cup TR_j) - CP_j$ , which is marked as the shaded area on the left in Fig. 2. Collisions are not entirely avoidable because VS is not empty. However, the large WS is a bigger problem.

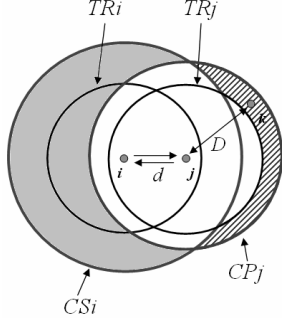


Figure 2. VS and WS in terms of CS, CP, and TR zone (VS: hatched area on the right, WS: shaded area on the left).

In our baseline model,  $z_0 = 10$  (or 10 dB) and  $\alpha = 4$ . Fig. 3(a) shows the case when  $d = 200\text{m}$ . We chose 200m because most of routing layer protocols provides communication distances as close to the maximum transmit distance, which is 250m in our example. Note that VS becomes negligible but a large WS may cause a serious performance problem. Note also that  $CS_i \supset TR_j$  which means that RTS/CTS handshake is not useful as also observed in [17, 18]. Now, consider the effect of short communication distance ( $d=100\text{m}$ ) on the WS. As shown in Fig. 3(b), the sender-receiver pair becomes more robust to interference, i.e.,  $CP_j$  becomes smaller and it results in an even larger WS.

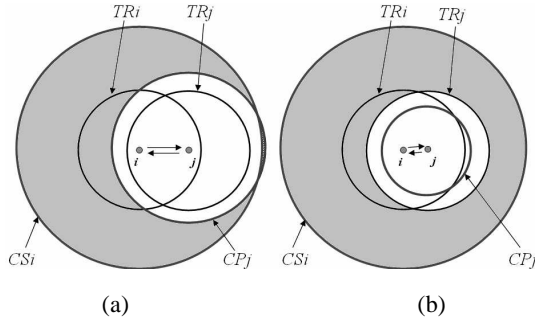


Figure 3. VS and WS when  $z_0 = 10$  dB and  $\alpha = 4$  (VS: empty, WS: large shaded area). (a)  $d = 200\text{m}$  and (b)  $d = 100\text{m}$ .

A straightforward solution to the large WS and the corresponding exposed terminal problem is to make  $CS_i$  small (or equivalently, increase the CS threshold). However, when  $d$  is large with a smaller  $CS_i$ , VS increases and the corresponding collision problem emerges. Therefore, it is imperative to have an adaptive capability that adjusts the CS threshold or the communication distance depending on the network state in the proximity.

## 4.2 Maximum Throughput with Multiple Interferers

Generally, there could be more than one interferer or equivalently, more than one senders, each of which interferes the

others. Therefore, the maximum total end-to-end throughput,  $T_e$ , is obtained when the number of senders that can simultaneously transfer data is maximized. Multiplying this number by the wireless link bandwidth and then dividing by the average number of hops between the source and the destination would give the estimate of  $T_e$ .

The number of senders can be maximized when the senders are located as close as possible but to the extent that each data transfer is not interfered by the rest of the senders. This is similar to the co-channel interference problem in cellular networks [21]. Consider the constellation of senders as in Fig. 4, which is the densest possible arrangement of senders. Assuming that each communication distance is  $d$ , our purpose is to find the sender-to-sender distance  $D$  that allows all data transfers to be simultaneously successful. We only consider the six first-tier interferers because the interference from them is much stronger than that from second-tier interferers and beyond. Now, the worst-case interference to the  $i$ - $j$  communication happens when the six interferers are  $(D - d)$ ,  $(D - d)$ ,  $(D - d/2)$ ,  $D$ ,  $(D + d/2)$ , and  $(D + d)$  apart to the receiver  $j$ , respectively [31]. Therefore, using equations (1) and (2),

$$SIR = \frac{d^{-\alpha}}{2(D-d)^{-\alpha} + (D-d/2)^{-\alpha} + D^{-\alpha} + (D+d/2)^{-\alpha} + (D+d)^{-\alpha}} > z_0 \quad (3)$$

If  $D_{\min}$  is the minimum  $D$  that satisfies equation (3), the maximum number of concurrent successful data transfers in a square network area of  $L \times L$  is

$$\frac{L}{D_{\min}} \times \frac{L}{\sqrt{3}/2 D_{\min}} = \frac{2L^2}{\sqrt{3}D_{\min}^2} \quad (4)$$

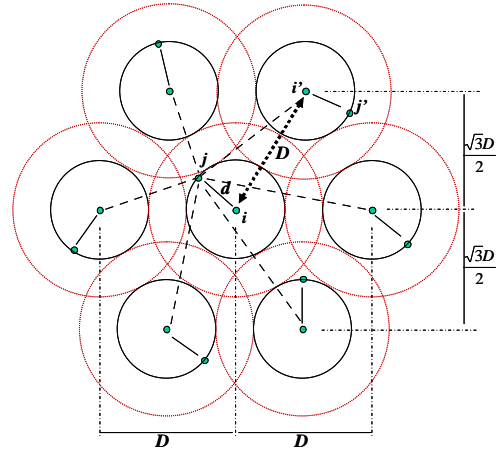


Figure 4. Constellation of senders for maximum throughput.

Since the average distance between a source-destination pair in the square network of  $L \times L$  is  $\sqrt{2}L/3$ , the average hop count is  $\sqrt{2}L/3d$ . Therefore,  $T_e$  is

$$T_e = \frac{2L^2b}{\sqrt{3}D_{\min}^2} + \frac{\sqrt{2}L}{3d} = \frac{\sqrt{6}Lbd}{D_{\min}^2} \text{ when } d_{CS} < D_{\min} \quad (5)$$

provided that the wireless communication bandwidth is  $b$  bits/second. Equation (5) becomes clearer if we make a simplifying assumption that the six interferers are all  $D$  apart from the receiver  $j$ . Then, equations (3) and (5) become

$$\frac{d^{-\alpha}}{6D_{\min}^{-\alpha}} = z_0, \text{ i.e. } D_{\min} = \sqrt[\alpha]{6z_0d} \quad (6)$$

and thus,

$$T_e = \frac{\sqrt{6Lbd}}{\left(\sqrt[\alpha]{6z_0d}\right)^2} = \frac{\sqrt{6Lb}}{\left(\sqrt[\alpha]{6z_0}\right)^2} \times \frac{1}{d} \text{ when } d_{CS} < D_{\min} \quad (7)$$

In other words,  $T_e$  increases as the communication distance  $d$  decreases as predicted in [8]. As an example, in the 915MHz WaveLAN radio hardware, the CS distance of 550m is considered optimal when communication distance is about 198m ( $= 550m/(6z_0)^{1/\alpha}$  when  $\alpha=4.0$  and  $z_0=10\text{dB}$ ).

Note that when  $d_{CS} \geq D_{\min}$ , each sender would be separated by  $d_{CS}$  instead of  $D_{\min}$  due to aggressive carrier sensing and thus, equation (5) becomes

$$T_e = \frac{\sqrt{6Lbd}}{d_{CS}^2} = \frac{\sqrt{6Lb}}{d_{CS}^2} \times d \text{ when } d_{CS} \geq D_{\min} \quad (8)$$

which means that  $T_e$  increases as the communication distance  $d$  increases.

Fig. 5 shows  $T_e$  versus  $d$  for different  $d_{CS}$  values based on equations (3), (5) and (8). Figs. 5(a) and 5(b) are for the path loss exponent,  $\alpha$ , of 2 and 4, respectively. When the path loss exponent is 2, the effect of communication distance is not significant. However, when it is 4 as in a land mobile environment, the effect becomes significant as in Fig. 5(b). From the  $d_{CS}$ 's point of view, when  $d_{CS}$  is large enough, it is better to exploit the CS-protected area and deliver data packets as far as possible within the CS zone (large communication distance  $d$ ). See mark (i) in Fig. 5(b). When  $d_{CS}$  is not large, we can obtain a better performance by shortening the communication distance even though it increases the hop count between the source and the destination (mark (ii)). From the communication distance's perspective, when short communications are frequent,  $D_{\min}$  required is smaller and equation (8) applies.  $T_e$  increases as  $d_{CS}$  decreases (or less sensitive carrier sensing) as indicated (iv) in the figure.

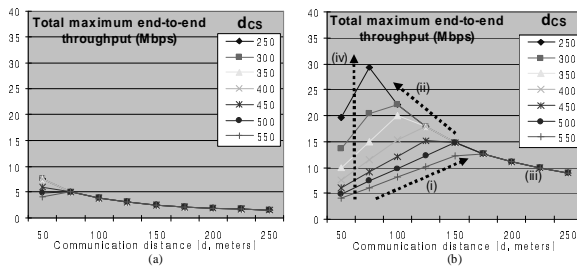


Figure 5. Maximum total end-to-end throughput ( $b=1\text{Mbps}$ ,  $L=10\text{km}$ ,  $z_0=10\text{dB}$ ). (a)  $\alpha=2.0$  and (b)  $\alpha=4.0$ .

The next section proposes a new MAC algorithm, which uses smaller  $d_{CS}$  and adjusts communication distance whenever necessary. Note that the CS threshold and  $d_{CS}$  is configurable

until it reaches the lowest boundary determined by the sensitivity of the carrier detect circuitry of the given radio hardware [14]. However, we adopt a smaller, fixed  $d_{CS}$  (350m) in the proposed scheme because the adaptive adjustment of this value would be complex [29].

## 5. MASA: HOP-BY-HOP MAC-LAYER SALVAGING

One important observation from the previous section is that the performance of a multihop network greatly depends on CS threshold and communication distance. This section proposes the *Multiple Access with Salvation Army (MASA)* protocol that uses a fixed, higher CS threshold (smaller  $d_{CS}$ ) to increase the spatial reusability and solves the collision problem from hidden terminals via packet salvaging at the link layer. It essentially reduces the communication distance on-the-fly by breaking one hop communication into two smaller-hop communications when it is beneficial. It is based on the DCF but does not use the optional RTS/CTS exchange because collisions in the absence of RTS/CTS can also be effectively masked by packet salvaging. The MASA algorithm includes two new frame types, called *SACK (Salvaging ACK)* and *SDATA (Salvaging DATA)* as will be explained later in this section. Throughout this paper, we assume to use PHY (physical layer) and MAC parameters of 915 MHz WaveLAN radio hardware [27], which are also used to derive default parameters in the ns-2 network simulator [4, 20].

### 5.1 Packet Salvaging in MASA

In wireless networks, nodes use broadcast as opposed to point-to-point communication and therefore data packets are typically sent to multiple nodes in the proximity of the sender at no extra cost. We call the set of those overhearing nodes the *salvation army*. A key idea in the proposed MASA protocol is that a third party node (say, node  $s$ ) in the salvation army captures or salvages a data packet that collided at the intended receiver and lets the packet make progress toward the receiver. This is drawn in Fig. 6(a). Since sender-salvager distance is smaller than sender-receiver distance, the salvager  $s$  receives the packet successfully with a higher probability and completes the communication session by replying SACK to node  $i$ . It then forwards the data packet (SDATA) to the original receiver  $j$  based on normal defer and backoff procedure. The corresponding messaging sequence is drawn in Fig. 6(b). Note that while ACK is transmitted regardless the status of the medium, SACK is transmitted only when the medium is free. This is to address the potential collision problem. The modified MAC behaviors at the salvager ( $s$ ), at the sender ( $i$ ) and at the receiver ( $j$ ) are described below.

First, at the sender ( $i$ ), when an ACK is not received during *ACKTimeout* interval, the sender concludes that the transmission has failed and invokes its backoff procedure to re-transmit the packet. In MASA, the sender cancels the backoff procedure when it receives SACK even after the *ACKTimeout* interval. Second, at the salvager ( $s$ ), it waits for a *SIFS (short inter-frame spacing)* [11] upon the successful reception of a data packet and checks the channel status (BUSY or IDLE), using the *clear channel assessment* or *CCA* signal supported in the IEEE 802.11 [11]. This is to determine whether it is necessary to salvage the packet or not. If ACK is received (more accurately, if

the channel status changes to BUSY), it cancels its salvaging activity. Otherwise, it starts its *salvaging backoff procedure*, explained shortly, and accordingly transmits SACK to the sender. Then, it starts its normal backoff procedure to forward the data packet (SDATA) to the receiver ( $j$ ) who then replies with an ACK to the salvager after an SIFS period. Both the sender and the salvager would retransmit the same packet for a specified number of times as defined in the DCF if they do not receive ACK or SACK. Third, at the receiver ( $j$ ), it may receive the same data packet more than once from more than one salvager. In the below, we explain how this problem is handled in MASA.

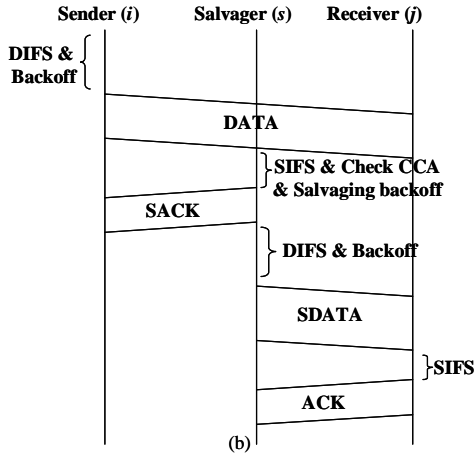
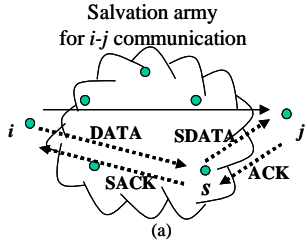


Figure 6. Salvation army and salvaging procedure. (a) Salvation army for  $i$ - $j$  communication, and (b) Salvaging procedure with SDATA/SACK.

It is possible that more than one node salvages the same packet and the receiver receives the same packet more than once. Such duplicate packets can be filtered out within the receiver MAC based on an original functionality of the DCF, called *duplicate packet filtering* [11]. This algorithm matches the sender address ( $Addr2$  in Fig. 7) and the sender-generated *sequence control number* ( $SC$ ) of a new packet against those of previously-received ones. If there is a match, the receiver transmits ACK but does not forward the packets. This does not solve the above mentioned problem in MASA because duplicate packets from different salvagers ( $s$  and  $t$ ) include different identities than node  $i$  in  $Addr2$  field. Our approach in MASA is to use a new data type SDATA that includes the original sender's address in  $Addr4$  (*logical address field*) so that the receiver can use this address rather than the salvager address ( $Addr2$ ) when it compares against the stored information.

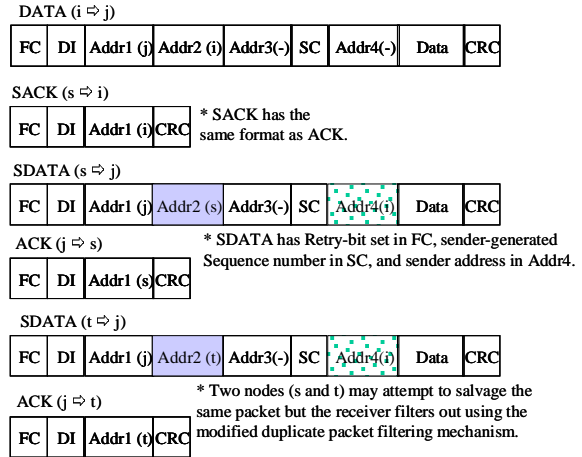


Figure 7. Format of MPDU frames in the MASA protocol (MPDU: MAC protocol data unit, FC: Frame control, DI: Duration/ Connection ID, SC: Sequence control).

## 5.2 Determination of a Salvager among Salvation Army

When more than one node is able to salvage a packet in collision, the candidate that can make the greatest progress should be selected. For this purpose, we assume that each node maintains neighbor list and signal quality information for its neighbors. It is not difficult to keep track of its neighbors because each node overhears every other neighbor's communications. The signal quality for each neighbor can be obtained using previous signal it received from the particular neighbor. We modify the functionality of PHY layer of IEEE 802.11 to support this. PHY layer of the IEEE 802.11 checks the *Received Signal Strength* (RSS) of the carrier to inform the channel status to the MAC layer (CCA signal) [11]. In MASA, we assume that the PHY layer informs not only the channel status but also the RSS information to the MAC. When a sender transmits a MAC frame, we assume that the frame includes the signal quality information for the receiver.

Now, when node  $s$  receives a data packet that is not intended for it, the node evaluates its eligibility as a salvager using the following rules. (i) The specified sender as well as the receiver must be in the neighbor list of node  $s$ . (ii) When node  $s$  overhears a SACK for the packet it is about to salvage, it should cancel its salvaging activity for that particular packet. (iii) In order for node  $s$  to make progress toward the receiver, it must be nearer to the receiver than the sender. Node  $s$  speculates this condition based on signal strength information as mentioned earlier. (iv) Node  $s$  must not have a pending packet at its MAC-layer software.

If a node is considered a legitimate candidate, it starts its salvaging activity at time  $t_0$  after waiting for an ACKTimeout interval as shown in Fig. 8. Then, it chooses its *salvaging backoff time* ( $t_s$ ) within the *salvaging interval* ( $T_{Si}$ ), during which it is allowed to salvage the packet.

- $T_{Si}$  can be considered the opportunity window open to salvagers, which starts at  $t_0$  and must end before the next data

transfer begins. Based on the operation principle of the DCF,  $T_{SI} = \text{ACK transmission time} + \text{DIFS}$  as shown in Fig. 8. This is because nodes in the proximity of the  $i$ - $j$  communication would wait for ACKTimeout for allowing the pair to complete their communication. An additional DIFS is available because it is required for a new data transfer to start. Nodes outside of  $TR_i$  may sense the erroneous packet and they would wait  $EIFS$  (*Extended IFS*) before starting their own transmission [11] but it turns out to offer the same opportunity window to salvagers because EIFS is set to  $SIFS + \text{ACK transmission time} + \text{DIFS}$  [11, 20]. The additional SIFS is taken care of because these nodes start their timer just after the data transmission. For simplicity, we do not include the propagation delay,  $\Delta$ , which is relatively small and can be ignored.

- $t_s$  is considered a priority among multiple candidates. A node that is closer to the receiver should be elected as the salvager because it can make a greater progress. The proposed MASA uses the signal quality to determine the salvager. In other words, node  $s$  calculates  $t_s$ , at which it transmits a SACK, using the signal quality from the sender ( $q_{is}$ ) and that from the receiver ( $q_{js}$ ), i.e.,  $t_s = q_{js}/q_{ji} \times T_{SI}$ . This is based on the assumption that the signal quality directly corresponds to distance. Even if the assumption is not valid, this arbitration rule simply becomes a randomized algorithm and it still works fine.

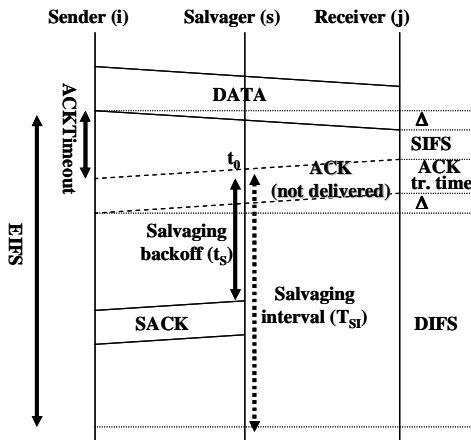


Figure 8. Distributed selection of a salvager ( $\Delta$ : propagation delay).

## 6. SIMULATION AND EVALUATION

In this section, the performance of the MASA algorithm is evaluated using the *ns-2* [20], which simulates node mobility, radio network interfaces, and the DCF protocol. The *two-ray ground propagation channel* is assumed with a radio transmission range of 250 m and a data rate of 2 Mbps. In order to show the benefit of the packet salvaging, Section 6.1 presents the simulation result of a simple 4- and 5-node scenario with a single interferer. More realistic scenarios with more than 50 nodes and the corresponding simulation results are presented in Sections 6.2 and 6.3, respectively.

### 6.1 Benefit of Packet Salvaging with a Single Interferer

Fig. 9 shows a simple communication scenario with 4 and 5 nodes. A node pair  $i$ - $j$  is our primary focus of interest while a node pair  $A$ - $B$  provides interfering signals. Node  $i$  sends 512-byte constant bit rate (CBR) or TCP packets to node  $j$ . Node  $A$  also sends 512-byte CBR or TCP packets to node  $B$ . In Direct scenario in Fig. 9(a), there exists no salvager candidate between nodes  $i$  and  $j$  and thus SIR at node  $j$  is always low and the communication is easily subjective to interference from node  $A$ . On the other hand, in Salvaging scenario in Fig. 9(b), node  $s$  is capable of capturing and salvaging a collided packet at node  $j$ . Thus, node  $j$  receives a stronger signal with high SIR from node  $s$ . Using equation (2), SIR at node  $j$  in Direct scenario is  $(400/250)^4$  or 8.16 dB for the packet from node  $i$ , which is smaller than  $z_0$ . But in Salvaging scenario, it is  $(400/160)^4$  or 15.92 dB for the packet that has been salvaged by  $s$ , which is larger than  $z_0$ .

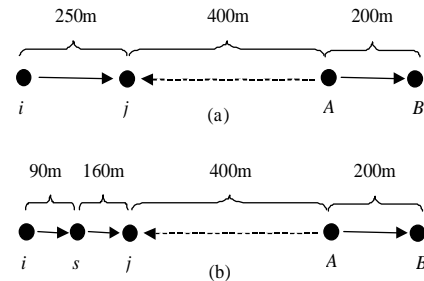


Figure 9. Simple communication scenario. (a) Direct and (b) Salvaging scenario.

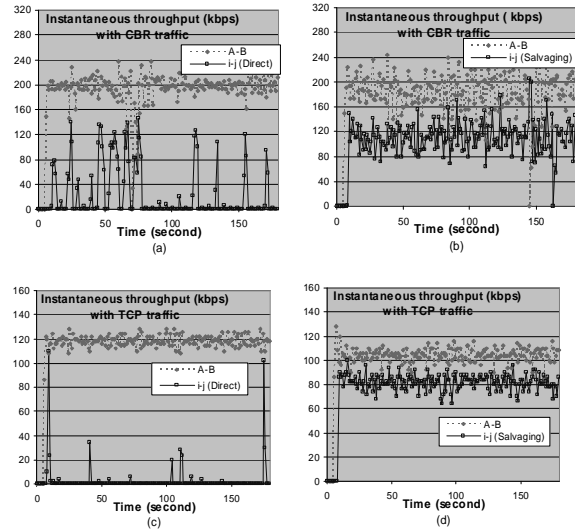


Figure 10. Capture effect and packet salvaging. (a) Direct with CBR traffic, (b) Salvaging with CBR traffic, (c) Direct with TCP traffic, and (d) Salvaging with TCP traffic.

Fig. 10 compares instantaneous throughput, measured at every simulated second, with CBR and TCP traffic. As shown in Figs. 10(a) and (b), the Salvaging scenario offers a higher aggregate throughput than the Direct scenario with CBR traffic even though

the average number of hops between the communication pair ( $i-j$ ) is larger. This is also true with TCP traffic as drawn in Figs. 10(c) and (d). Moreover, the Direct scenario exhibits unacceptably serious unfairness, which is a well-researched phenomenon observed by Xu *et al.* [30]. According to their observation, the throughput of one TCP session can be almost zero while the other TCP session monopolizes the channel bandwidth. Our simulation results confirm that this is also the case with CBR traffic and infer that the capture effect and packet salvaging may alleviate the fairness as well as the performance problem.

## 6.2 Simulation Environment with Multiple Interferers

The previous section shows the benefit of packet salvaging in MASA on a small network with a single interferer. The following two sections present the merits of the proposed MASA algorithm in more complex and larger network scenarios. Protocols to be compared are MASA, DCF2 (DCF without RTS/CTS) and DCF4 (DCF with RTS/CTS). We included DCF2 because MASA does not incorporate the RTS/CTS handshake, either. Note that DCF2 in general outperforms DCF4, which is counter-intuitive but has been predicted by a number of researchers [17, 18] and also discussed in Section 2 in this paper. This is mainly due to the overly sensitive CS threshold. In other words, RTS/CTS handshake simply adds MAC control overhead with little gain. One interesting observation we have made, however, is DCF2 degrades more significantly in comparison to DCF4 with the *shadowing radio-propagation model*. Randomness in radio propagation makes the RTS/CTS handshake more useful. We will discuss this issue later in Section 6.3.

Our evaluation is based on the simulation of 100 mobile nodes located in an area of  $300 \times 1500 \text{ m}^2$ . The CS distance is assumed to be 550m and 350m with the DCF and the MASA, respectively. AODV routing algorithm [22] is used to find and maintain the routes between two end-nodes. The data traffic simulated is CBR and TCP traffic. In case of CBR, 40 sources generate three 256-byte data packets every second. Destination nodes are selected randomly. The *random waypoint mobility model* is used in our experiments with the maximum node speed of 5 m/s and the pause time of 100 seconds. Simulation time is 900 seconds and each simulation scenario is repeated ten times to obtain steady-state performance metrics. For more accurate performance evaluation, we also used different routing algorithm (DSR [12]), and different propagation model. Various traffic intensities in terms of packet rate and the number of sources and various numbers of nodes are also used to see the performance scalability of the DCF and the MASA.

In our experiments, we assume the followings regarding signal capture.

- First, when two packets arrive, if the first signal is 10dB ( $\alpha_0$ ) stronger than the second, then the first signal can be successfully received. However, if the second signal is 10dB stronger than the first, neither packet is successful because the receiving node already starts decoding the first signal and cannot switch to the second immediately. This is actually the way the ns-2 is implemented. However, in the latter case, if

the first signal is weaker than the receive threshold but larger than CS threshold, the receiver can receive the second signal successfully. Since ns-2 still drops both packets in this case, we modified ns-2 to reflect this fact.

- Second, the SIR computation requires two samples of the signal, the desired signal and the signal with interference, and we assume that they are available for computation.
- Third, the signal strength comparison for determining capturing is on a per-packet basis in ns-2. That is, if multiple interfering packets were to be received, they are only compared individually, not their combinations. We modified ns-2 to simulate additive interference if there exist concurrent multiple interfering signals.

## 6.3 Results and Discussion

Fig. 11 shows the network performance with respect to node mobility represented by pause time. Note that 900 seconds of pause time means a static scenario while 0 second of pause time means a constant-moving scenario. Figs. 11(a) and (b) show the *packet delivery ratio (PDR)* and packet delay with CBR traffic. While the PDR of MASA is on par with that of DCF2 as shown in Fig. 11(a), it is clear from Fig. 11(b) that MASA outperforms DCF2 and DCF4 in terms of packet delay, which is 53~85% and 59~86% reduction, respectively. There are two major factors that contribute to reduction of the packet delay. First, the proposed MASA algorithm induces fewer false alarms for live links. Each link error report in AODV triggers an expensive route-discovery procedure causing the packet in transit as well as the following packets to experience a large packet delay until a new routing path is found. It also causes network-wide flooding of RREQ packets that waste a substantial amount of wireless bandwidth.

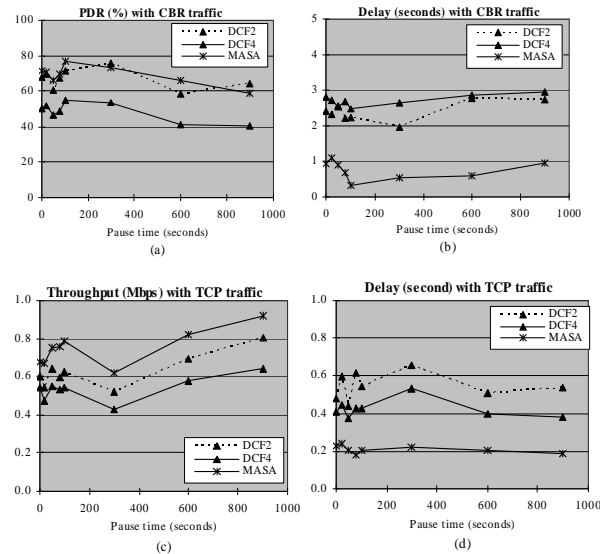


Figure 11. Performance comparison with different mobility. (a) Packet delivery ratio, (b) Packet delay with CBR traffic, (c) Throughput and (d) Response time with TCP traffic.

The large reduction in packet delay with the CBR traffic motivated us to experiment with TCP traffic because TCP

behaves adaptively according to *round trip time (RTT)* estimate. We simulated 40 TCP connections in the same ad hoc network environment. The aggregate end-to-end throughput and response time are reported in Figs. 11(c) and (d), respectively. As shown in the figure, the MASA achieves as much as 27% and 45% higher throughput compared to DCF2 and DCF4. Response time reduces as much as 70% and 58% as seen in Fig. 11(d). It is concluded from Fig. 11 that the MASA protocol and its MAC-layer packet salvaging mechanism in general improves the network performance, particularly for TCP-based applications. More importantly, the MASA would be best suited in application scenarios where delay is a primary concern.

An interesting observation with this simulation result is that performance degrades as node mobility decreases (during 100~900 seconds with CBR traffic in Figs. 11(a) and (b), and during 100-300 seconds with TCP traffic as drawn in Figs. 11(c) and (d)). The same phenomenon was also reported in [5] and the authors explained that this is due to a higher level of network congestion and multiple access interferences at certain regions of the ad hoc network. With moderate node mobility, every node experiences overloading when it happens to be in the center but the trouble disappears when it moves away from the center. With less mobility, the same set of nodes in the center keeps overloaded and thus, they become serious bottlenecks in the network. However, as no mobility decreases even further, link errors are reduced significantly and thus the negative effect is cancelled out. When additive interference is considered as explained in the previous subsection, overloading would be more significant and the corresponding negative effect continues well beyond the case of unmodified ns-2 simulation without additive interference. For comparison purpose, Fig. 12 shows the simulation result with unmodified ns-2. We used the same set of simulation parameters as used for experiments in Fig. 11. As clearly seen from the figure, additive interference decreases PDR as much as 20%, which suggests the importance of realistic simulation.

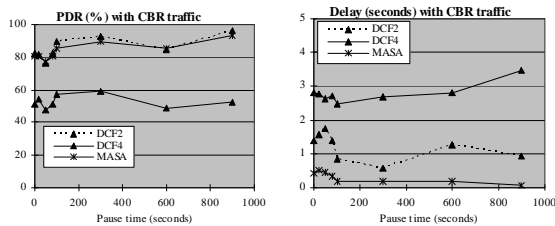


Figure 12. Simulation result (PDR and packet delay) using unmodified ns-2 without additive interference.

In order to see the main causes of the performance improvement as well as to enhance the MASA algorithm even further, routing overhead, data overhead and packet queue size have been measured during the simulation. Fig. 13 provides the overhead analysis with TCP traffic. As in Fig. 13(a), DCF2 and DCF4 generate more than 3.4 and 4.1 times many routing control packets (RREQ, RREP, and RERR) than MASA, respectively. (It is 1.3 and 7.1 with CBR traffic.) At pause time of 900 seconds where mobile nodes are static and thus no RERR packets are expected, DCF2 and DCF4 still result in 1106 and 1083 RERR packets which must be contrasted to 413 such

packets with MASA. In terms of normalized control overhead, MASA employs 0.27~0.36 control packets per successfully-delivered data packet, while it is 0.59~1.22 and 0.72~1.48 with DCF2 and DCF4, respectively. Making progress with packet salvaging in the MASA algorithm reduces false alarms more than half in spite of network congestion and thus reduces the routing control overhead significantly.

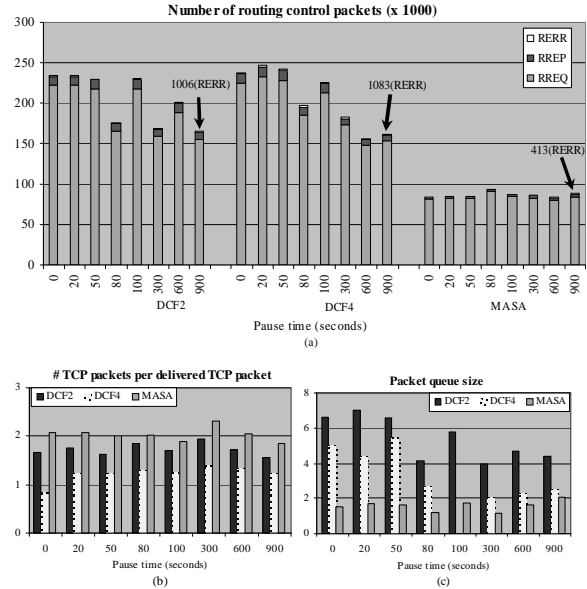


Figure 13. Overhead analysis with TCP traffic. (a) Routing overhead, (b) Normalized data overhead and (c) Packet queue size.

However, as far as the data transmission overhead is concerned, the MASA is disadvantageous. Fig. 13(b) shows that the number of TCP packets transmitted at the MAC layer for each successfully-delivered TCP packet. They are 1.65, 0.84, and 2.08 data packets for DCF2, DCF4, and the MASA, respectively, with the pause time of 0 second. Since the DCF4 algorithm employs the RTS/CTS exchange before transmitting a data packet, it results in fewer collisions on data packets and thus reduces the data transmission overhead compared to DCF2 and MASA. In comparison to DCF2, the MASA algorithm generates more overhead mainly because of the reduced CS zone. Nonetheless, it does not overshadow the advantage of the MASA algorithm as already shown in Fig. 11.

As discussed earlier, a primary advantage of MASA is short packet delay. Our investigation shows that packet queuing delay is an important ingredient for this. Once again, making progress via packet salvaging facilitates a mobile node to quickly offload pending packets and therefore, it helps keep its packet queue at the routing layer as short as possible. In each of 900 seconds of simulation runs, we collected the information of packet queue size every 10 seconds at each node and calculated the average statistics across all mobile nodes in the network. As seen in Fig. 13(c), each node has about 5.39 and 3.06 packets in its queue on average with DCF2 and DCF4, respectively, while it is 1.57 with MASA. Similar observations have been made with CBR traffic. One thing to note is that control overhead of DCF2

and DCF4 is much more significant than MASA with CBR traffic (normalized control overhead is 3.1 and 6.7 times higher than MASA).

Scalability of the three protocols is compared with larger number of communication pairs (connections) and various numbers of nodes. Figs. 14(a) and (b) show the PDR and throughput with different numbers of CBR and TCP connections, respectively. For CBR traffic, we used the packet rate of 2 packets/second. It can be inferred from the figures, particularly from Fig. 14(b), that the proposed MASA consistently outperforms DCF2 and DCF4 regardless of the traffic intensity. In fact, the advantage of the MASA becomes more pronounced as the number of connections increases. This is because the MASA encourages more spatial reuse and thus is more beneficial if backlogged nodes can be found in any of the reusable spatial area.

More number of nodes is especially helpful in MASA as shown in Figs. 14(c) and (d). Since DCF2 and DCF4 cause more route-discoveries with RREQ flooding, more number of nodes directly translates to the exponential increase of routing control overhead. Fig. 14(c) shows the PDR comparison among the three protocols. The MASA performs consistently better irrespective the number of nodes but DCF2 and DCF4 degrade significantly. Since TCP sources adapt their data rate based on network feedback, the corresponding performance is somewhat controlled as shown in Fig. 14(d). However, MASA still outperforms DCF2 and DCF4.

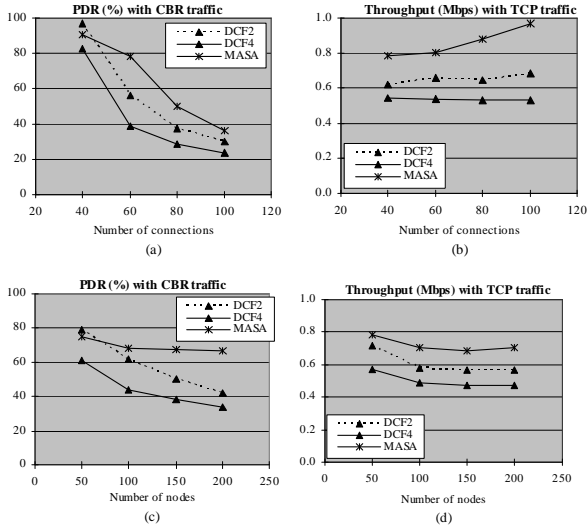


Figure 14. Scalability comparison. (a) Effect of traffic intensity with CBR traffic and (b) with TCP traffic, (c) Effect of node density with CBR traffic and (d) with TCP traffic.

We have also studied several other interesting scenarios including those with different routing protocol and different radio propagation model. One of the main differentiating characteristics of the proposed MASA protocol is its independence of upper layer protocols. Figs. 15(a) and (b) show the performance evaluation with a different routing algorithm, DSR. 40 CBR sources generate 1~5 packets every second in this simulation. The simulation results show that the performance advantage of the MASA is consistent regardless the routing algorithm employed at the network layer. Next, Figs. 15(c) and

(d) present the simulation results with shadowing propagation model with AODV routing algorithm and CBR traffic. Shadowing causes slow variations over the mean received power which is usually lognormally distributed and thus provides random variation in radio propagation, which is in fact more realistic than two-ray ground model. The MASA is more advantageous mainly due to its adaptive capability. Since DCF2 and DCF4 behave depending on deterministic distance based on RTS, CTS and carrier sense coverage, they would suffer more when wireless links are more random.

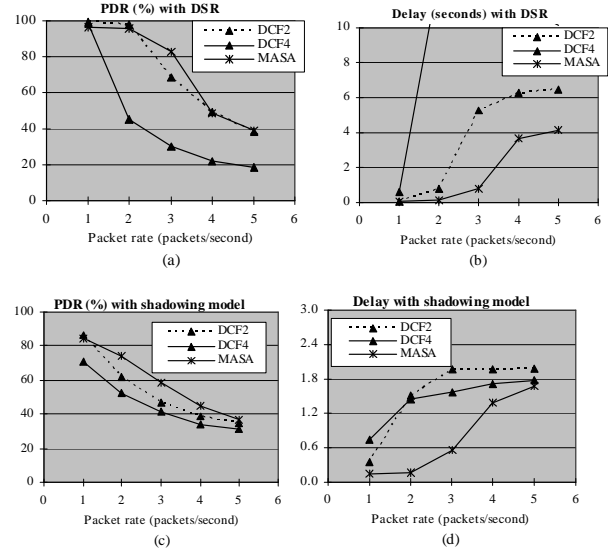


Figure 15. Effect of system parameters. (a) PDR with DSR and (b) Delay with DSR, (c) PDR with shadowing model, and (d) Delay with shadowing model.

## 7. CONCLUSION AND FUTURE WORK

Carrier sensing MAC protocols avoid collisions by employing aggressive carrier sensing but it makes them unable to maximize the spatial spectral utilization. This paper analyzes the upper bound throughput of a carrier sensing MAC and observes that the network throughput can be greatly improved if the capture effect is taken into consideration.

The proposed MASA algorithm adopts a fixed, small carrier sense range but adaptively adjusts the communication distance via salvaging packets. While the former increases spatial reusability, the latter alleviates the collision problem. For practicality, we considered implementation of MASA based on the DCF specification. Our extensive simulation study showed that MASA enhances the network performance regardless of mobility, traffic intensity and the routing algorithm used. In particular, it reduces packet delay significantly.

The MASA algorithm is considered the most preferable in a wireless ad hoc network where a large number of nodes exchange small packets, which is typically the case in *wireless sensor networks*. The application of MASA in this important area comprises our future work. Another future work is to elect a salvager deterministically rather than randomly between each pair of communicating nodes.

## 8. REFERENCES

- [1] Bertsekas, B., and Gallager, R. Multiaccess Communication. Ch. 4, *Data Networks*, 2<sup>nd</sup> Edition, Prentice Hall PTR, Upper Saddle River, New Jersey, 1992.
- [2] Biswas, S., and Morris, R. Opportunistic Routing in Multi-Hop Wireless Networks. *The Second Workshop on Hot Topics in Networking (HotNets-II)*, 2003.
- [3] Blum, B., He, T., Son, S., and Stankovic, J. IGF: A State-Free Robust Communication Protocol for Wireless Sensor Networks. *Technical Report CS-2003-11*, Dept. Computer Science, University of Virginia, April 21, 2003.
- [4] Bonsall, A., Wang, D., and Stancil, D. D. Propagation Model Embedded in a Wireless Network Simulator. *The 3<sup>rd</sup> Annual Wireless Communications Conference*, 1998.
- [5] Das, S. R., Perkins, C. E., Royer, E. M. Performance Comparison of Two On-Demand Routing Protocols for Ad Hoc Networks. *IEEE INFOCOM*, 2000.
- [6] De Couto, D. S. J., Aguayo, D., Chambers, B. A., and Morris, R. Performance of Multihop Wireless Networks: Shortest Path is Not Enough. *The First Workshop on Hot Topics in Networks (HotNets-I)*, 2002.
- [7] Goldsmith, A. J., Wicker, S. B. Design Challenges for Energy-Constrained Ad Hoc Wireless Networks. *IEEE Wireless Communications*, 2002, 8-27.
- [8] Grossglauser, M., and Tse, D. Mobility Increases the Capacity of Ad-hoc Wireless Networks. *IEEE INFOCOM*, 2001.
- [9] Gupta, P., and Kumar, P. R. The Capacity of Wireless Networks. *IEEE Trans. Information Theory*, 46(2), Mar. 2000, 388-404.
- [10] He, T., Stankovic, J. A., Lu, C., and Abdelzaher, T. F. SPEED: A Stateless Protocol for Real-Time Communication in Sensor Networks. *IEEE ICDCS*, May 2003.
- [11] IEEE Std 802.11-1999, Local and Metropolitan Area Network, Part 11: Wireless LAN Medium Access Control and Physical Layer Specifications, <http://standards.ieee.org/getieee802/download/802.11-1999.pdf>.
- [12] Johnson, D. B., and Maltz, D. Dynamic Source Routing in Ad-Hoc Wireless Networks. Ch. 5, *Mobile Computing*, edited by Imielinski, T., and Korth, H., Kluwer Academic Publishers, 1996, 153-181.
- [13] Jung, E.-S., and Vaidya, N. H. A Power Control MAC Protocol for Ad Hoc Networks. *IEEE/ACM MobiCom*, 2002.
- [14] Kamerman, A., and Monteban, L. WaveLAN-II: A High-Performance Wireless LAN for the Unlicensed Band. *Bell Labs Technical Journal*, Summer 1997, 118-133.
- [15] Karp, B. Geographic Routing for Wireless Networks. Ph.D. Dissertation, Harvard University, October, 2000.
- [16] Kleinrock, L., and Tabagi, F. A. Packet Switching in Radio Channels: Part I – Carrier Sense Multiple-Access Models and Their Throughput-Delay Characteristics. *IEEE Trans. Communications*, (23)12, Dec. 1975.
- [17] Miller, L. E. Carrier Sense Threshold/Range Control: Compilation of MANET email messages,” <http://www.antd.nist.gov/wctg/manet/docs/carriersense.pdf>, Jan. 2004.
- [18] Mühlethaler, P., and Najid, A. Throughput optimization in multihop CSMA mobile adhoc networks. *European Wireless Conference*, 2004.
- [19] Narayanaswamy, S., Kawadia, V., Sreenivas, R. S., and Kumar, P. R. Power Control in Ad-Hoc Networks: Theory, Architecture, Algorithm and Implementation of the COMPOW Protocol. *European Wireless Conference*, 2002, 156-162.
- [20] ns-2 Network Simulator, <http://www.isi.edu/nsnam/ns/>.
- [21] Pahlavan, K., and Krishnamurthy, P. Network Planning. Ch. 5, *Principles of Wireless Networks*, Prentice Hall PTR, Upper Saddle River, New Jersey, 2002.
- [22] Perkins, C. E., and Royer, E. Ad-hoc On-Demand Distance Vector Routing. *IEEE Workshop on Mobile Computing Systems and Applications*, 1999, 90-100.
- [23] Prabhakar, B., Uysal-Biyikoglu, E., and El Gamal, A. Energy-efficient Transmission over a Wireless Link via Lazy Packet Scheduling. *IEEE INFOCOM*, 2001, 386-394.
- [24] Sadeghi, B., Kanodia, V., Sabharwal, A., and Knightly, E. Opportunistic media access for multirate ad hoc networks. *IEEE/ACM MobiCom*, 2002.
- [25] Shepard, T. J. A Channel Access Scheme for Large Dense Packet Radio Networks. *ACM SIGCOMM*, 1996.
- [26] Skraba, P., Aghajan, H., and Bahai, A. Distributed Passive Routing Decisions in Mobile Ad-Hoc Networks. *IEEE Vehicular technology Conference (VTC'04)*, Sept. 2004.
- [27] Tuch, B. Development of WaveLAN, an ISM Wireless LAN. *AT&T Technical Journal*, 72(4), Jul./Aug. 1993, 27-37.
- [28] Valera, A., Seah, W., and Rao, S. V. Cooperative Packet Caching and Shortest Multipath Routing In Mobile Ad hoc Networks. *IEEE INFOCOM*, 2003.
- [29] Xu, K., Gerla, M., and Bae, S. Effectiveness of RTS/CTS handshake in IEEE 802.11 based adhoc networks. *Ad Hoc Network Journal*, 1(1), July 2003, 107-123.
- [30] Xu, S., and Saadawi, T. Does the IEEE 802.11 MAC Protocol Work Well in Multihop Wireless Ad Hoc Networks? *IEEE Communications Magazine*, Jun. 2001, 130-137.
- [31] Yang, X., and Vaidya, N. On the Physical Carrier Sense in Wireless Ad Hoc Networks. Technical Report, University of Illinois at Urbana-Champaign, July 2004.
- [32] Ye, F., Yi, S., and Sikdar, B. Improving Spatial reuse of IEEE 802.11 Based Ad Hoc Networks. *IEEE GLOBECOM*, 2003.
- [33] Yu, C., Shin, K. G., and Lee, B. Power-Stepped Protocol: Enhancing Spatial Utilization in a Clustered Mobile Ad Hoc Network. *IEEE Journal on Selected Areas in Communications (J-SAC)*, 22(7), Sep. 2004, 1322-1334.
- [34] Zhu, J., Guo, Yang, L. L., and Conner, W. S. Leveraging Spatial Reuse in 802.11 Mesh Networks with Enhanced Physical Carrier Sensing. *IEEE ICC'04*, 2004.
- [35] Zorzi, M., and Rao, R. Capture and retransmission control in mobile radio. *IEEE Journal on Selected Areas in Communications*, 12(8), 1994, 1289-1298.
- [36] Zorzi, M., and Rao, R. Geographic Random Forwarding (GeRaF) for ad hoc and sensor networks: energy and latency performance. *IEEE Tran. Mobile Computing*, 2(4), 2003.